

POSSIBLE SUBGROUPS OF GLOBULAR CLUSTERS AND PLANETARY NEBULAE IN NGC 5128

KRISTIN A. WOODLEY

Department of Physics & Astronomy, University of British Columbia, Vancouver BC V6T 1Z1, Canada

WILLIAM E. HARRIS

Department of Physics & Astronomy, McMaster University, Hamilton ON L8S 4M1, Canada

Draft version October 5, 2018

ABSTRACT

We use recently compiled position and velocity data for the globular cluster and planetary nebula subsystems in NGC 5128, the nearby giant elliptical, to search for evidence of past dwarf-satellite accretion events. Beyond a $10'$ (~ 11 kpc) radius in galactocentric distance, we find tentative evidence for 4 subgroups of globular clusters and 4 subgroups of planetary nebulae. These each have > 4 members within a search radius of $2'$ and internal velocity dispersion of $\lesssim 40$ km s⁻¹, typical parameters for a dwarf galaxy. In addition, 2 of the globular cluster groupings overlap with 2 of the planetary nebulae groupings, and 2 subgroupings also appear to overlap with previously known arc and shell features in the halo light. Simulation tests of our procedure indicate that the probability of finding false groups due to chance is $< 1\%$.

Subject headings: galaxies: elliptical and lenticular, cD — galaxies: individual (NGC 5128) — galaxies: interactions — galaxies: star clusters — globular clusters: general — planetary nebulae : general

1. INTRODUCTION

In the last decade or so, the presence of stellar streams within nearby galaxies has provided direct evidence for the continual build-up of massive galaxies from the accretion of small neighbouring satellites. For example, in the Milky Way, there is the Sagittarius stream (Ibata et al. 1997, 2001a; Majewski et al. 2003; Martínez-Delgado et al. 2004), and in M31, a number of new streams have been recently discovered within the *Pan-Andromeda Archeological Survey* (McConnachie et al. 2009), adding to the list of already known streams in that galaxy (Ibata et al. 2001b). As well, striking surface brightness features tracing a galaxy's merger history have been found in NGC 5907 (Shang et al. 1998), NGC 891 (Mouhcine et al. 2010a), NGC 4093 (Martínez-Delgado et al. 2008), NGC 253 and NGC 5236 (Malin & Hadley 1997), and UGC 10214 (Forbes et al. 2003), among others. Past work has shown that it is possible to use streams to trace the orbits of satellite galaxies that had merged with the Milky Way in the distant past (Lynden-Bell & Lynden-Bell 1995; Yoon & Lee 2002). Lynden-Bell & Lynden-Bell (1995) suggest that the tidal debris stripped out of the parent dwarf galaxy will not undergo much dynamical friction because its mass content will be low.

In systems beyond our Local Group galaxies, finding these traces of old satellites becomes more difficult. But in addition to the field-star integrated light, it is possible to use other old objects such as globular clusters (GCs) and planetary nebulae (PNe) to provide evidence for the presence of accretion remnants (Forte et al. 1982; Muzzio 1987; Côté et al. 1998, 2002; Hilker et al. 1999). As well, Pipino et al. (2007) have modelled the GC as-

sembly history in massive galaxies, and showed that in addition to the GCs that formed along with the galaxy halo, a significant fraction of GCs that make up the massive galaxies were likely accreted from dwarf galaxies in later times. Indeed, subgroups of GCs have been found within the halos of massive galaxies or have been associated with the stellar streams in the Sagittarius stream (Ibata et al. 1994, 1997; Bellazzini et al. 2003) and in M31 (Perrett et al. 2003; Mackey et al. 2010).

For our search, we target NGC 5128 (Centaurus A) which is a giant elliptical galaxy at a distance of 3.8 ± 0.1 Mpc (Harris et al. 2010a). While this galaxy is quite close, it is still beyond the distance where detecting faint stellar streams is an easy task. Previous work by Malin et al. (1983) and Peng et al. (2002) has shown there are existing complex shell structures that surrounds the central regions out to 15 kpc, attributed to the many accretions of small neighbouring galaxies. There are also HI shells (Schiminovich et al. 1994) and a prominent warped dust lane (Graham 1979) is also present in the central region where gas and dust is settling into the central potential well. There is evidence for young stars (Rejkuba et al. 2001, 2002; Ellis et al. 2009) that may be aligned with the radio jet. This star formation could have been triggered by the jet colliding with cloud material brought into NGC 5128 via a merging event.

NGC 5128 has 607 confirmed GCs, via radial velocity measurements (van den Bergh et al. 1981; Hesser et al. 1984, 1986; Harris et al. 1992; Peng et al. 2004b; Woodley et al. 2005; Rejkuba et al. 2007; Beasley et al. 2008; Woodley et al. 2010a,b) and/or resolved images from the *Advanced Camera for Surveys* on the *Hubble Space Telescope* (Harris et al. 2006; Mouhcine et al. 2010b). Of these, 563 have measured radial velocities. Their mean measurement uncertainty is 42 km s⁻¹, though the range of uncertainties is quite large, with

96% of the population having uncertainties $< 200 \text{ km s}^{-1}$. The currently knowns GCs are distributed in galactocentric radius out to $50'$ (where $1' \sim 1.1 \text{ kpc}$ at the distance of NGC 5128), although the inner $5'$ is sparsely populated because of the obscuration of the well known central dustlane. There are also 780 confirmed PNe with positional and radial velocity data (Peng et al. 2004a), which can be used as stellar tracers in the same way.

2. GROUP IDENTIFICATION TECHNIQUE

2.1. Globular Cluster Observational Dataset

From both the GC and PNe databases, we attempt to identify genuine subgroups in the classic way by looking for objects that are close to each other in both position and velocity. Our basic search approach follows that of Perrett et al. (2003) for the GCs in M31. We look first at the GCs. Here the NGC 5128 GC data face us with the additional difficulty beyond the situation in M31: not only are the positions and velocities seen only in projection, but the velocity measurement uncertainties (averaging more than 40 km s^{-1}) are usually larger than the expected $\sim 20 \text{ km s}^{-1}$ true, physical velocity dispersion of a typical satellite dwarf in the Local Group (Geha et al. 2010). For this reason, we view our present work as only a preliminary step towards finding genuine physical subgroups. For the same reason, we suggest that at this stage, only rather simple group-finding search procedures are justified. Logical next steps would include higher-precision velocity data, and imaging to search for faint surface brightness features.

GC metallicity or color might in principle be additional search criteria, as it may be expected that GCs within one accreted system may share similar enrichment processes, but these properties are less useful in practice. In our sample of GCs, the metallicities are either from a color transformation or simply based on a color division which we take from Woodley et al. (2007, 2010a,b). We have classified the GCs as being either metal-poor or blue ($[Fe/H] < -1.0$) or as metal-rich or red ($[Fe/H] \geq -1.0$) following previous work on the GC system of NGC 5128 (Harris et al. 2004b; Woodley et al. 2005, 2007) or as metal-rich or red if $(B - I) \geq 2.072$ and metal-poor or blue if $(B - I) < 2.072$, following Peng et al. (2004b). The division between red and blue GCs is thus not homogeneously determined and depends on a variety of methods as well as a number of different photometric studies. Of these GCs, 291 are classified as metal-poor, 292 as metal-rich, and 24 GCs have insufficient photometry for any of the above transformations. In addition, while there is evidence that the metallicities, on average, of GCs in dwarf galaxies are more metal-poor than in more massive galaxies (Sharina et al. 2010), there is evidence that a range of metallicities of GCs can exist within a single dwarf galaxy, for example, in the dwarf galaxies IC10 and UGCA86 (Sharina et al. 2010). As well, there can exist a spread in the metallicities of the dwarf galaxies themselves (see the review of Mateo 1998). This information, taken together, makes it quite difficult to incorporate a defined range of acceptable color or metallicity within a subgroup as a search parameter (we note that Perrett et al. (2003) also ignored metallicity as a search parameter).

We searched for GC subgroups in the outer regions of

NGC 5128, beyond $10'$. Inside this radius, there would be a high fraction of false subgroups because the density of objects is high, and the biggest source of finding false subgroups is due to the accidental 2-dimensional projection of objects that are actually far apart along the light of sight. Additionally, it is the outer halo that should still preserve coherent traces of accreted satellites because the much larger dynamical times there prevent them from being fully phase-mixed (Bullock & Johnston 2005).

As mentioned above, we use essentially a nearest-neighbour approach with two linking criteria. For each GC outside a $10'$ galactocentric distance, we calculate the separation in projected linear distance between it and all other GCs in the catalog (the boundary can therefore extend slightly inwards of $10'$) and group the GCs if these are within our imposed linking length. We also included the GC velocity and velocity uncertainties in our search such that two GCs would match if the range of its velocity plus or minus its velocity uncertainty can be subtracted from another objects velocity such that their absolute difference is less than 20 km s^{-1} . For example, objects with velocities $500 \pm 30 \text{ km s}^{-1}$ and $460 \pm 20 \text{ km s}^{-1}$ would be linked. To help avoid false group detections based on poorly measured velocities, we only considered GCs whose velocity uncertainties were less than an imposed limit. We also combined groups that were found to have common members, which allows for groups that may exist in a chain-like structure.

A search using a spatial linking length of $1'$ did not yield any subgroups with more than 4 members. When we increased the linking length to $2'$, which is a reasonable size for a subgroup from a dwarf galaxy, we did indeed find plausible subgroups. With a linking length of $2'$, as well as allowing for velocity uncertainties of up to 40 km s^{-1} , we have detected a plausible subgroup of GCs including 6 group members. When we include GCs in our search that have measured velocity uncertainties up to 50 km s^{-1} , we increase the number of group members by 1, and call this a possible group of 7 members, labelled GC 1. When we increase the allowed velocity uncertainty to 80 km s^{-1} , we end up finding 3 additional subgroups, each consisting of 5 members, which we label groups GC 2, GC 3, and GC 4. Many of these are likely to be included simply because of the large velocity allowance and we cannot be sure that these are all real groups. If we set our velocity uncertainty limit to 40 km s^{-1} , but increase our linking length to $3'$, we increase the number of members in our subgroup from 6 to 10 (included as possible members of group GC 1). Many of these included GCs may not be real members. The possible subgroups are plotted in Figure 1 and are listed in Table 1 with columns of the GC ID, group ID, *R.A.* and *Decl.* in J2000 coordinates, the $[Fe/H]$ value, their galactocentric radius, R_{gc} , and their measured radial velocity, v_r , and associated uncertainty, σ_{v_r} . The radial velocities and uncertainties are weighted values determined from all previous measurements in the literature. These values are obtained from Woodley et al. (2007), Woodley et al. (2010a) and Woodley et al. (2010b).

The image of NGC 5128 in Figure 1 was obtained with the *Mosaic II* optical CCD camera on the 4 meter *Blanco* telescope at the *Cerro Tololo Inter-American Observatory*. It was provided to us in its reduced form graciously

by Eric Peng with its reduction described in Peng et al. (2002). We have smoothed the image using a 300×300 pixel box and subtracted it from the original image. To enhance the visibility of the low-surface brightness shells and arc structures and preserve some of the dominant bulge light, we added back 15% of the smoothed image. We find that in a general sense, the candidate subgroups that we have identified fall in the same radial zones of galactocentric distance where the shells are found. However, a stronger indication of possible connections is seen along the isophotal major axis of the galaxy (35° and 215° E of N, Dufour et al. (1979)). Toward the southeast (lower right in Figure 1), group GC 1 falls on the irregular plume of light, while on the opposite side to the northwest, group GC 3 falls on or close to the two of the visible arcs. The remaining two groups, GC 2 and GC 4, do not seem to be projected on any known surface brightness features.

2.2. Planetary Nebula Observational Dataset

We have performed the same subgroup finding algorithm on the available PNe data in the literature. There are 780 PNe with radial velocity measurements (Peng et al. 2004a; Hui et al. 1995) in NGC 5128, which have been detected by the [OIII] emission line. While there are no velocity uncertainties presented in the literature for the PNe, we have assumed a radial velocity uncertainty of 20 km s^{-1} for each object, which is the typical *rms* velocity error presented in Peng et al. (2004a). Using our same subgroup finding criteria as for the GCs (linking length of $2'$, velocity difference of 20 km s^{-1} plus the inclusion of the velocity uncertainties, at a minimum distance of $10'$ from the center of the galaxy for the central group member), we have found 4 potential groups. These groups are plotted in Figure 1 and listed in Table 2 which provides their ID from Peng et al. (2004a), their group ID, *R.A.* and *Decl.* in J2000 coordinates, the galactocentric radius, R_{gc} , their radial velocity measurement, v_r , and assumed 20 km s^{-1} velocity uncertainty. Out of the 4 subgroups of PNe discovered, 3 have group sizes of 5–6, while the remaining group has 9 members. These groups have been labelled PNe 1, PNe 2, PNe 3, and PNe 4.

2.3. Properties of Subgroups

The mean velocity and *rms* velocity dispersions for each group are listed in Table 3. The velocity dispersion for each subgroup ranges from $29 - 43 \text{ km s}^{-1}$ for the GC subgroups and from $12 - 24 \text{ km s}^{-1}$ for the PNe subgroups, within a reasonable range for a plausible group.

Our results indicate there are 3 possible overlaps between the GC and the PN subgroups. These are PNe 1 with GC 2 (Group 1), PNe 2 with GC 3 (Group 2), and PNe 3 with GC 4 (Group 3). Examining the average velocities for each of these subgroups, the average radial velocity differences are $\Delta(\langle v_{GC} \rangle - \langle v_{PNe} \rangle) = 39 \text{ km s}^{-1}$ for Group 1, -136 km s^{-1} for Group 2, and 0 km s^{-1} for Group 3. The difference in average velocities for Group 1 and Group 3 are within the expected uncertainty range of the measured velocities, which is 42 km s^{-1} for the average GC. The subgroups of Group 2, however, do not appear to have strong velocity connections, and are likely either not real groups or are overlapping

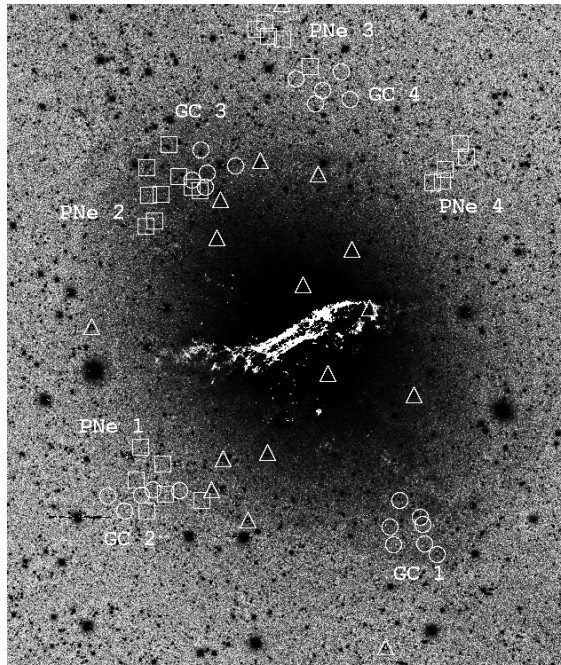


FIG. 1.— We show the positions of the potential groups of GCs and planetary nebulae in NGC 5128. The group labelled GC 1 (circles) are the 7 members found with a linking length of $2'$ with allowed velocity uncertainties of 50 km s^{-1} . We also plot the 3 additional GC subgroups that are found when GCs with velocity uncertainties of up to 80 km s^{-1} are included, labelled GC 2, GC 3 and GC 4 (circles). The 4 plausible PNe subgroups are also shown, groups PNe 1, PNe 2, PNe 3 (note one PNe is off the plot), and PNe 4 (squares). The locations of the friendless PNe determined in Section 4 with $N = 10$ and $\sigma_N = 3$ (see text for a detailed description of these parameters) are also plotted (triangles). The image of NGC 5128 is $\sim 25'$ across with North up and East to the left, and objects in the outer regions are not shown (see text).

by chance in projection. In Sections 2.4 & 3.3, we analyze the probability that the overlapping can occur by chance.

In very rough terms we can estimate the total luminosity of the underlying satellite galaxy that would consist of either ~ 6 GCs or 6 PNe, typical of what we have found in our subgroups. Considering first the GC subgroups, we *assume* a specific frequency, S_N , which is the number of GCs per unit $M_V = -15$ galaxy luminosity (Harris & van den Bergh 1981). We adopt $S_N = 3$, typical for a normal faint galaxy, though note that Peng et al. (2008) show that the range of S_N for dwarf galaxies spans 1-20. With these inputs, we obtain $M_V = -15.8$ mag and a surface brightness of $24 \text{ mag per arcsec}^2$ assuming the galaxy is spherically shaped with a $2'$ radial extent. For a PN subgroup of ~ 6 members, we can estimate the bolometric luminosity of the underlying satellite galaxy with the luminosity specific PN number, $\alpha = N_{PN}/L_{tot}$, where N_{PN} is the total number of PNe and L_{tot} is the total luminosity (Jacoby 1980). Ciardullo et al. (2005) shows $\alpha_{0.5} \sim 2 \times 10^{-9}$ for galaxies in the range of $M_B \sim -14$ to -16 (please see their Figure 1). However, in the case of NGC 5128, the PNe data extend at least 1.5 mag down the luminosity function (Peng et al. 2004a), and we thus estimate $\alpha_{1.5} \sim 11.5 \times 10^{-9}$, to obtain $L_{tot} = 5.2 \times 10^8 L_\odot$. We obtain $M_V = -16.2$ mag after a bolometric correction of -0.85 (Buzzoni et al. 2006). Assuming the galaxy is spherical with a radial extent of

$2'$, we obtain a surface brightness of 24 mag per arcsec². Both estimates of the surface brightness of a potential underlying dwarf galaxy are very rough guides due to the input assumptions, and we do not think this test is capable of ruling out whether or not we should see these structures in previously obtained deep images of NGC 5128. We appear to be finding mild traces of substructure that are not hugely above the statistical noise.

2.4. Scrambling the Velocities

Our first step towards assessing how real our candidate groups in Table 1 are is through a non-parametric test. By taking our GC positions in 2-dimensional space, we randomly assign each GC a unique and real velocity and velocity uncertainty from the GC catalog. We then perform our search for subgroups with a linking length of $2'$, a velocity difference of 20 km s^{-1} plus the inclusion of velocity uncertainties up to 40 km s^{-1} , at a minimum distance of $10'$ from the center of the galaxy for the central group member. Out of 1000 trials, we found that 23.2% of cases found one group containing at least 4 members. In 1.8% of the cases, the trials found 2 groups with at least 4 members, and in 1 case (0.1%), there were 3 groups found. This indicates that it is likely that one of the GC candidate subgroups may be a false group. We did not find a case, however, in which 4 candidate groups arose with this methodology.

We examined closely the groups in this test that had more than one group per trial. In the 18 cases that found 2 groups, there were 2 trials in which the groups overlapped in projected space. In the trial consisting of 3 groups, 2 of these groups overlapped. This indicates, that while finding more than 1 group in a trial was rare, when it did occur, there was an approximate 15% chance they would overlap. Since these groups were all from the GC population, none of the subgroups that overlapped had similar average radial velocities.

Finally, we randomly assigned each GC a unique and real velocity and velocity uncertainty from the GC catalog, but this time, we incorporated GCs with velocity uncertainties up to 80 km s^{-1} . Our results indicate that out of 1000 trials, at least 4 false groups were found in 1.5% of the cases. This simple test indicates that it is not likely that *all* 4 GC subgroups are false, but it is quite probable that some may indeed be false.

3. SIMULATING GLOBULAR CLUSTER SYSTEMS

3.1. Searching for False Subgroups

Here, we assess how often our search procedure would turn up false groups of similar apparent quality from purely random distributions. It is similarly important to examine how often our procedure would successfully find a real subgroup within the data.

To carry out tests of the procedure, we generated simulated GC systems in which the particles are located randomly within a spherically symmetric space distribution following a 3-dimensional density power law $\rho \sim r^{-n}$, with $n(3D) = 2.5$ for the metal-poor GCs and $n(3D) = 3.0$ for the metal-rich clusters. The particle velocities were assigned randomly in a Gaussian distribution with a dispersion of 150 km s^{-1} for all GCs, and their individual measurement uncertainties were randomly distributed uniformly from $5 - 80 \text{ km s}^{-1}$. All of these parameters mimic the NGC 5128 GC system.

For 1000 realizations, each GC system consisted of 550 objects, with 50% red and 50% blue subpopulations, which were projected from their real 3-dimensional positions into 2-dimensions. We then searched for subgroups with our finding algorithm, as we have done for the observational data in Section 2.1. Our search criteria allowed objects to be group members only if they were within a projected length of $2'$ from each other, have a velocity difference of $< 20 \text{ km s}^{-1}$, exist outside of $10'$ from the galaxy's center, and have a velocity uncertainty less than 40 km s^{-1} for each member. Allowing the higher velocity uncertainty limit than imposed in most of our observational searches of 40 km s^{-1} will only overestimate the number of false group members we find in the simulations. Out of the 1000 trials, 9 of them detected one subgroup. The subgroups consisted of 5-7 members. This test therefore suggests that there is a 0.9% chance of detecting a false group from our observationally mimicked dataset.

We further this work by generating a GC system that has 1300 GCs, which is the total estimated population in NGC 5128 (Harris 2010b). Our simulated system has 650 blue and 650 red clusters, projected into 2-dimensions. In the observed GC system, there are 242 objects beyond our inner search radius of $10'$ so we randomly selected 242 objects beyond $10'$ from our simulated sample of 1300 GCs. We repeated our group finding algorithm to this simulated system as described above. This simulation represents the most realistic system we can make to match our observed dataset. Out of our 1000 simulations, there were 3 trials that detected a subgroup of GCs, each of these groups consisted of 5 members, suggesting that we would find a fake subgroup of GCs with a 0.3% chance. Both this simulation, as well as our simulated group of 550 objects show that the probability of finding one fake subgroup of GCs in a system similar to our observed dataset is $< 1\%$. None of the trials detected more than one subgroup in the simulation.

3.2. The Addition of Real Subgroups

It is important to also check how reliable our subgroup finding technique is at recovering a real group in our observed system. This was tested by inserting a real subgroup into one of our simulations of 1300 members where no fake subgroup was found. We generated 1000 real groups by randomly selecting their position in x, y, and z in the galaxy, as well as their velocity and velocity uncertainty. Each real subgroup had between 4-6 members with a group velocity dispersion of within 20 km s^{-1} . Their individual velocities were selected from a system with 150 km s^{-1} dispersion. The group was inserted between $10-50'$ from the galaxy's center which ensures the real group should be present in the projected system in our search regime. The differences in the x and y and z positions for the group members was selected within $2'$ of each other.

Out of the 1000 simulations that we performed, 892 of these simulations found all group members and no fake interlopers. All real group members were recovered as well as the inclusion of fake members in 103 of the simulations. In 2 of the simulations, some of the real group members were found with fake member interlopers, and in 3 of the simulations some of the group members were found with no fake interlopers detected. We therefore

consider our detection method to be very successful as in more than $> 89\%$ of cases, we were able to find our exact simulation group system and 10.3% of the time, we also found all group members however with interlopers. When interlopers were present in the detected subgroups, 96.2% of these occurrences had only 1 interloper, while 2 interlopers were detected in the remaining cases. These results strongly suggest that at least some of our observationally detected subgroups are real and they cannot all simultaneously be false detections.

3.3. Testing for the Probability of Random Overlapping Groups

Lastly, we test whether our candidate subgroups might be smaller ones overlapped by projection purely by chance. To the simulated GC system as a whole, we add random subgroups consisting of 4-6 members whose members are confined within a $2'$ region. These subgroups were randomly placed in the galaxy between 10 - $50'$ before being deprojected into 2-dimensional space. Two groups were considered to overlap if any one of their members were within a small designated distance from any member of another group. The distance chosen did not significantly change our findings (considering differences between $0.1 - 2'$), so we selected $0.5'$.

We performed 7 simulations, each consisting of a different number of subgroups placed in the galaxy, which increased linearly from 2 subgroups up to 8 subgroups. For each of these simulations, we examined, over 1000 trials, how many times these subgroups overlapped. The number of overlaps ranged from no overlapping subgroups up to 5 overlapping subgroups. We did not find any simulation which had more than 5 overlapping groups. As would be expected, the higher the number of subgroups present, the higher the number of overlapping subgroups are found as a result. These probabilities of having random overlapping groups are listed in Table 4. We find that the probability of having two subgroups randomly overlap is $\sim 4\%$. If all 8 subgroups in NGC 5128 (4 GCs and 4 PNe) are real groups, then the probability that 3 sets of subgroups randomly overlap is found to be $\sim 7\%$. Excluding Group 2, whose subgroups have very different average velocities, our results suggest there may be 2 sets of overlapping subgroups, Group 1 and Group 3. The probability of 2 sets of subgroups randomly overlapping with 8 subgroups present is 23% . It is therefore not clear if these overlapping subgroups found in Groups 1 and 3 are real.

4. SEARCHING FOR STELLAR ORBITS

Work by Peng et al. (2002) shows a complex but faint shell structure threading the inner and mid-halo regions of NGC 5128. These shells have been attributed to the phase-wrapping of stars from accreted satellites. One particular blue elliptical arc was found to be associated with a young star clusters ($\simeq 350$ Myr), but aside from this one example, no stellar streams have been associated with GCs or PNe.

We have begun a search for evidence of stellar streams in NGC 5128 by probing the objects within the galaxy that may trace the stream. We use the available data for the GCs and the PNe, which may be stripped along with the stellar stream material during galaxy interactions. If these objects are located, they can be used to identify the

possible orbits of accreted satellites. To do this, we use a friendless algorithm (Merrett et al. 2003) and search for evidence of stellar streams using the GCs and PNe separately in the analysis below.

For each object in our sample with a measured radial velocity and a velocity uncertainty less than 50 km s^{-1} (totalling 411 GCs and 780 PNe), we have found its N nearest neighbours. For those N neighbours, we have calculated their mean velocity $v_{mean,N}$ and their velocity dispersion, σ_N . We have classified the central object as friendless if its velocity is more than $n \times \sigma_N$ from $v_{mean,N}$. Varying the N parameter does not seem to significantly alter the results. We do find varying the σ_N parameter from 3 to 4 changes the number of friendless objects by a few, while varying σ_N from 2 to 3 does change the number of objects significantly.

Taking a conservative approach and using $\sigma_N = 4$, we find no friendless GCs when $N = 30$, 1 when $N = 20$ (GC0258), and 1 when $N = 10$ (GC0578). GC0258 will not be considered further as it was classified as a resolved GC in Harris et al. (2006) while a recent radial velocity measurement indicates this object may be a star (Woodley et al. 2010b), and it is because of this low radial velocity measurement that this object is identified. GC0578 may indeed be friendless, but it is not possible to use one GC to indicate evidence for a stellar stream. Using $N = 10$ and $\sigma_N = 3$ yields 7 friendless GCs (GC0216, GC0249, GC0325, GC0506, GC0577, GC0578, GC0580).

We conduct the same analysis with the PNe dataset using $\sigma_N = 4$ and find no friendless objects when $N = 30$, 1 when $N = 20$ (f05p02), and 6 when $N = 10$ (4012, 4285, 5602, f05p02, f18p28, f42p10). Using $N = 10$ and $\sigma_N = 3$ yields 20 friendless PNe (4012, 4128, 4285, 4417, 4511, 5203, 5601, 5602, 5617, 6104, f04p1, f05p02, f08p50=3002, f14p016, f18p28, f18p65=1208, f18p67=4023, f18p83, f42p10, mosNEpn4). The locations of the inner ~ 15 of these are shown in Figure 1.

The friendless objects that are located at the largest distances from the galaxy's center are likely not indicators of streams. Rather, there are very few neighbours as the incompleteness of planetary nebulae and GCs is quite high beyond $20'$ (see the radial distribution as a function of azimuth for the GCs in Figure 8 of Woodley et al. (2010b) and the distribution of the PN in Figure 2 of Peng et al. (2004a)). This leaves only the inner $20'$ which can be explored for friendless objects, of which there are few (again, depending on the parameters chosen in the friendless algorithm). We list these objects with the suggestion that (at least) some of them may trace stellar orbits, and continued searches for stellar streams or orbital modelling are necessary to go beyond this preliminary work.

5. CONCLUSIONS

We have searched the GC and PN systems in the nearby giant elliptical galaxy, NGC 5128, for evidence of stellar subgroups and stellar streams from merging events. Our results indicate there may be up to 4 potential subgroups of GCs and 4 potential subgroups of PNe. Two of the PNe subgroups overlap with two of the GC subgroups in position and velocity. In order to improve the search for these subgroups in NGC 5128, we need higher precision radial velocity measurements to more concretely determine if these objects are grouped

together.

By generating GC systems that mimic that in NGC 5128, we are able to assign the probability of our results being a chance encounter due to the projection of these objects onto a 2-dimensional plane. The probability of finding a fake subgroup within the GC population is $< 1\%$, while the probability of having a set of subgroups overlap is $\sim 4\%$. These results strongly suggest that at least some of these subgroups may indeed be real.

We have also searched for evidence of stellar streams by locating GCs and planetary nebulae that differ from its neighbours in velocity space using a friendless search

algorithm. We present our findings as potential tracers, however further work in orbital modelling as well as searches for very faint surface brightness features would be necessary beyond this point to further define the stellar streams.

K.A.W. thanks Dr. Harvey Richer and W.E.H. thanks NSERC for their financial support. K.A.W. and W.E.H. thank Dr. Eric Peng for providing the image of NGC 5128 in Figure 1.

REFERENCES

- Ashman, K. M. & Bird, C. M. 1993, *AJ*, 106, 2281
 Beasley, M. A., Bridges, T., Peng, E. W., Harris, W. E., Harris, G. L. H., Forbes, D. A., & Mackie, G. 2008, *MNRAS*, 386, 1443
 Bellazzini, M., Ferraro, F. R., & Ibata, R. A. 2003, *AJ*, 125, 188
 Bullock, J. S. & Johnston, K. V. 2005, *ApJ*, 635, 931
 Buzzoni, A., Arnaboldi, M., & Corradi, R. L. M. 2006, *MNRAS*, 368, 877
 Ciardullo, R., Sigurdsson, S., Feldmeier, J. J., & Jacoby, G. H. 2005, *ApJ*, 629, 499
 Côté, P., Marzke, R. O., & West, M. J. 1998, *ApJ*, 501, 554
 Côté, P., West, M. J., & Marzke, R. O. 2002, *ApJ*, 567, 853
 Dufour, R. J., van den Bergh, S., Harvel, C. A., Martins, D. H., Schiffer, F. H., Talbot, R. J., Talent, D. L., & Wells, D. C. 1979, *AJ*, 84, 284
 Ellis, S. et al. 2009, The Many Faces of Cen A, Conference
 Forbes, D. A., Beasley, M. A., Bekki, K., Brodie, J. P., & Strader, J. 2003, *Science*, 301, 1217
 Forte, J. C., Martínez, R. E., & Muzzio, J. C. 1982, *AJ*, 87, 1465
 Geha, M., van der Marel, R. P., Guhathurta, P., Gilbert, K. M., Kalirai, J., & Kirby, E. N. 2010, *ApJ*, 711, 361
 Graham, J. A. 1979, *ApJ*, 232, 60
 Harris, W. E., & van den Bergh, S. 1981, *AJ*, 86, 1627
 Harris, G. L. H., Geisler, D., Harris, H. C., & Hesser, J. E. *AJ*, 104, 613
 Harris, W. E. & Harris, G. L. H. 2002, *AJ*, 123, 3108
 Harris, G. L. H., Harris, W. E., & Geisler, D. 2004b, *AJ*, 128, 723
 Harris, W. E., Harris, G. L. H., Barmby, P., McLaughlin, D. E., & Forbes, D. A., 2006, *AJ*, 132, 2187
 Harris, G. L. H., Rejkuba, M. & Harris, W. E. 2010a, *arXiv0911.3180*
 Harris, G. L. H. 2010b, *arXiv1004.4907*
 Hesser, J. E., Harris, H. C., van den Bergh, S., & Harris, G. L. H. 1984, *ApJ*, 276, 491
 Hesser, J. E., Harris, H. C., & Harris, G. L. H. *ApJ*, 303, L51
 Hilker, M., Infante, L., & Richtler, T. 1999, *A&AS*, 138, 55
 Hui, X., Ford, H. C., Freeman, K. C., & Dopita, M. A. 1995, *ApJ*, 449, 592
 Ibata, R. A., Gilmore, G., & Irwin, M. J. 1994, *Nature*, 370, 194
 Ibata, R. A., Wyse, R. F. G., Gilmore, G., Irwin, M. J., & Suntzeff, N. B. 1997, *AJ*, 113, 634
 Ibata, R. A., Lewis, G. F., Irwin, M., Totten, E., & Quinn, T. 2001a, *ApJ*, 551, 294
 Ibata, R. A., Irwin, M., Lewis, G., Ferguson, A. M. N., & Tanvir, N. 2001b, *Nature*, 412, 49
 Jacoby G., 1980, *ApJS*, 42, 1
 Lynden-Bell, D. & Lynden-Bell, R. M. 1995, *MNRAS*, 275, 429
 Mackey, D. et al. 2010 (in prep)
 Majewski, S. R., Skrutskie, M. F., Weinberg, M. D., & Ostheimer, J. C. 2003, *ApJ*, 599, 1082
 Malin, D. F., Quinn, P. J., & Graham, J. A. 1983, *ApJ*, 272, 5
- Malin, D. & Hadley, B. 1997, *PASA*, 14, 52
 Martínez-Delgado, D., Gómez-Flechoso, M. A., Aparicio, A., & Carrera, R. 2004, *ApJ*, 601, 242
 Martínez-Delgado, D., Peñarrubia, J., Gabany, R. J., Trujillo, I., Majewski, S. R., & Pohlen, M., 2008, *ApJ*, 689, 184
 Mateo, M. L. 1998, *ARA&A*, 36, 435
 McConnachie, A. W. et al. 2009, *Nature*, 461, 66
 Merrett, H. R., Kuijken, K., Merrifield, M. R., Romanowsky, A. J., Douglas, N. G., Napolitano, N. R., Arnaboldi, M., Capaccioli, M., Freeman, K. C., Gerhard, O., Evans, N. W., Wilkinson, M. I., Halliday, C., Bridges, T. J., & Carter, D. 2003, *MNRAS*, 346, L62
 Mouhcine, M., Harris, W. E., Ibata, R., & Rejkuba, M. 2010b, *MNRAS*, 404, 1157
 Mouhcine, M., Ibata, R., & Rejkuba, M. 2010a, *ApJ*, 714, 12
 Muzzio, J. C. 1987, *PASP*, 99, 245
 Peng, E. W., Ford, H. C., Freeman, K. C. & White, R. L. 2002, *AJ*, 124, 3144
 Peng, E. W., Ford, H. C., & Freeman, K. C. 2004a, *ApJ*, 602, 685
 Peng, E. W., Ford, H. C., & Freeman, K. C. 2004b, *ApJ*, 602, 705
 Peng, E. W., Jordán, A., Côté, P., Takamiya, M., West, M. J., Blakeslee, J. P., Chen, C.-W., Ferrarese, L., Mei, S., Tonry, J. L., & West, A. A. 2008, *ApJ*, 681, 197
 Perrett, K. M., Stiff, D. A., Hanes, D. A., & Bridges, T. J. 2003, *ApJ*, 589, 790
 Pipino, A., Puzia, T. H., & Matteucci, F. 2007, *ApJ*, 665, 295
 Reed, L. G., Harris, G. L. H., & Harris, W. E. 1994, *AJ*, 107, 555
 Rejkuba, M., Minniti, D., Silva, D. R., & Bedding, T. R. 2001, *A&A*, 379, 781
 Rejkuba, M., Minniti, D., Courbin, F., & Silva, D. R. 2002, *ApJ*, 564, 688
 Rejkuba, M., Dubath, P., Minniti, D., & Meylan, G. 2007, *A&A*, 469, 147
 Schiminovich, D., van Gorkum, J. H., van der Hulst, J. M., & Kasow, S. 1994, *ApJ*, 423, L101
 Shang, Z., et al. 1998, *ApJ*, 504, L23
 Sharina, M. E., Chandar, R., Puzia, T. H., Goudfrooij, P., & Davoust, E. 2010, *MNRAS*, tmp, 536 (NEED VOLUME)
 van den Bergh, S., Hesser, J. E., & Harris, G. L. H. 1981, *AJ*, 86, 24
 Woodley, K. A., Harris, W. E. & Harris, G. L. H. 2005, *AJ*, 129, 2654
 Woodley, K. A., Harris, W. E., Beasley, M. A., Peng, E. W., Bridges, T. J., Forbes, D. A., & Harris, G. L. H. 2007, *AJ*, 134, 494
 Woodley, K. A., Harris, W. E., Puzia, T. H., Gómez, M., Harris, G. L. H., & Geisler, D. 2010a, *ApJ*, 708, 1335
 Woodley, K. A., Gómez, M., Harris, W. E., Geisler, D., & Harris, G. L. H., 2010b, *AJ*, 139, 1871
 Yoon, S.-J. & Lee, Y.-W. 2002, *Science*, 297, 578

TABLE 1
POSSIBLE GLOBULAR CLUSTER SUBGROUPS IN NGC 5128

ID	Group ID	<i>R.A.</i> (<i>J</i> 2000)	<i>Decl.</i> (<i>J</i> 2000)	[<i>Fe/H</i>]	<i>R_{gc}</i> (<i>l</i>)	<i>v_r</i> (km s ⁻¹)	<i>σ_{v_r}^c</i> (km s ⁻¹)
GC0067	GC 1	13:24:51.49	-43:12:11.1	-1.17	12.86	624	13
GC0083	GC 1	13:24:56.08	-43:10:16.4	-2.46	10.79	687	31
GC0106	GC 1	13:25:01.83	-43:09:25.4	-1.42	9.52	688	16
GC0114 ^a	GC 1	13:25:03.37	-43:11:39.6	-1.29	11.41	605	46
GC0117	GC 1	13:25:04.48	-43:10:48.4	-0.32	10.54	626	22
GC0122 ^b	GC 1	13:25:05.46	-43:14:02.6	-1.37	13.51	679	13
GC0419	GC 1	13:24:55.31	-43:10:39.3	-0.35	11.19	656	27
GC0422 ^b	GC 1	13:25:03.28	-43:08:14.4	-1.65	8.37	690	31
GC0491	GC 1	13:24:54.98	-43:11:36.9	-0.22	12.05	670	19
GC0492 ^b	GC 1	13:24:56.61	-43:12:23.6	-1.94	12.59	713	28
GC0504 ^b	GC 1	13:25:08.94	-43:08:53.7	-1.96	8.46	678	26
GC0354	GC 2	13:26:02.25	-43:08:55.6	-0.65	10.03	457	38
GC0598	GC 2	13:26:09.52	-43:08:52.4	-0.41	10.88	482	67
GC0379	GC 2	13:26:12.82	-43:09:09.2	-0.49	11.50	545	60
GC0544	GC 2	13:26:17.27	-43:09:58.0	-0.05	12.65	473	39
GC0393	GC 2	13:26:22.08	-43:09:10.7	-1.20	12.79	505	78
GC0534	GC 3	13:25:55.35	-42:53:40.2	-2.30	9.04	347	41
GC0590	GC 3	13:25:46.96	-42:52:34.0	-0.95	9.28	355	66
GC0532	GC 3	13:25:54.79	-42:52:57.1	-0.33	9.59	399	32
GC0341	GC 3	13:25:58.91	-42:53:18.9	-1.34	9.70	410	20
GC0334	GC 3	13:25:56.59	-42:51:46.6	-0.73	10.77	403	16
GC0518	GC 4	13:25:25.36	-42:49:27.5	-1.55	11.70	589	63
GC0163	GC 4	13:25:15.79	-42:49:15.1	-1.44	12.09	534	52
GC0516	GC 4	13:25:23.31	-42:48:47.7	-0.54	12.38	526	11
GC0220	GC 4	13:25:30.72	-42:48:13.4	-1.88	12.94	484	47
GC0511	GC 4	13:25:18.29	-42:47:52.4	-0.65	13.39	487	39

^a Included if velocity uncertainty cut-off increased from 40 km s⁻¹ to 50 km s⁻¹.

^b Included member in group if linking length increased from 2' to 3'.

TABLE 2
POSSIBLE PLANETARY NEBULAE SUBGROUPS IN NGC 5128

ID	Group ID	<i>R.A.</i> (<i>J</i> 2000)	<i>Decl.</i> (<i>J</i> 2000)	<i>R_{gc}</i> (<i>l</i>)	<i>v_r</i> (km s ⁻¹)	<i>σ_{v_r}^a</i> (km s ⁻¹) ^a
ctr513	PNe 1	13:26:14.26	-43:08:22.5	11.18	480	20
f08p10=5506	PNe 1	13:26:06.19	-43:09:06.2	10.63	462	20
5508	PNe 1	13:26:13.01	-43:06:45.0	10.01	439	20
f07p06	PNe 1	13:26:11.33	-43:09:57.3	11.89	421	20
f07p08	PNe 1	13:26:06.87	-43:07:36.0	9.65	476	20
f08p9	PNe 1	13:25:56.04	-43:09:24.7	9.76	439	20
f17p34	PNe 2	13:26:11.29	-42:52:39.6	11.65	535	20
f18p46	PNe 2	13:26:10.83	-42:54:01.5	10.64	527	20
f18p51	PNe 2	13:26:07.42	-42:54:01.4	10.18	530	20
f18p55=1217	PNe 2	13:26:02.57	-42:53:07.1	10.26	516	20
f18p74=1303	PNe 2	13:26:05.35	-42:51:31.3	11.84	522	20
5106	PNe 2	13:26:11.57	-42:55:37.7	9.75	506	20
5108	PNe 2	13:26:09.16	-42:55:20.1	9.56	513	20
f18p69=4031	PNe 2	13:25:56.78	-42:53:50.4	9.05	499	20
f18p70	PNe 2	13:25:58.98	-42:53:39.0	9.44	517	20
f18p15	PNe 3	13:25:41.55	-42:45:41.5	15.67	519	20
f18p16	PNe 3	13:25:38.18	-42:46:04.4	15.20	501	20
f18p17	PNe 3	13:25:39.18	-42:45:24.2	15.89	534	20
f18p18	PNe 3	13:25:34.32	-42:46:11.5	15.01	531	20
f18p40	PNe 3	13:25:40.29	-42:43:44.0	17.57	553	20
f18p26	PNe 3	13:25:26.79	-42:47:36.5	13.54	507	20
ctr624	PNe 4	13:24:50.38	-42:53:22.6	10.33	557	20
f19p06	PNe 4	13:24:45.76	-42:51:30.0	12.31	588	20
f19p07	PNe 4	13:24:44.04	-42:52:09.9	12.01	538	20
4608	PNe 4	13:24:49.87	-42:52:46.8	10.85	597	20
ctr622	PNe 4	13:24:53.26	-42:53:26.8	9.94	566	20

^a For all PNe, we have assumed a radial velocity uncertainty of 20 km s⁻¹.

TABLE 3
PROPERTIES OF THE SUBGROUPS

Group ID	v_{mean} (km s ⁻¹)	σ (km s ⁻¹)
GC 1 ^a	651	25
GC 2	492	26
GC 3	382	19
GC 4	524	34
PNe 1	453	21
PNe 2	518	11
PNe 3	524	17
PNe 4	569	21

^a These values have been calculated using the 7 probably group members of GC 1 using a linking length of 2'.

TABLE 4
CHANCE OF OVERLAPPING SUBGROUPS

N Subgroups	N Occurances out of 1000					
	0 overlaps	1 overlap	2 overlaps	3 overlaps	4 overlaps	5 overlaps
2	958	42	0	0	0	0
3	869	129	2	0	0	0
4	783	213	4	0	0	0
5	631	327	40	2	0	0
6	439	450	99	11	1	0
7	358	445	160	36	1	0
8	249	441	229	67	13	1